American Journal of Medical Genetics Part A

WILEY

AMERICAN JOURNAL OF medical genetics PART A

ORIGINAL ARTICLE

ATP6V0A2-Related Cutis Laxa: Identification of a Recurrent Exon 16 Deletion With Founder Effect in Southeastern Türkiye and a Novel Frameshift Variant

Zeynep Esener[1] | Murat Öztürk[2] | Esra Habiloğlu[2] | Aysel Tekmenuray-Ünal[3] | Gül Ünsel-Bolat[4] | Figen Eşmeli[5] | Abdullah Sezer[6] | Edanur Bulut[1] | Hilmi Bolat[1]

[1]Department of Medical Genetics, Faculty of Medicine, Balikesir University, Balikesir, Türkiye | [2]Department of Medical Genetics, Batman Training and Research Hospital Batman, Batman, Türkiye | [3]Department of Medical Genetics, Antalya Education and Research Hospital, Antalya, Türkiye | [4]Department of Child and Adolescent Psychiatry, Faculty of Medicine, Balıkesir University, Balikesir, Türkiye | [5]Department of Neurology, Faculty of Medicine, Balikesir University, Balikesir, Türkiye | [6]Department of Medical Genetics, Etlik City Hospital, Ankara, Türkiye

Correspondence: Zeynep Esener (zeynepesenermd@gmail.com)

Received: 22 October 2025 | **Revised:** 10 February 2026 | **Accepted:** 14 February 2026

Keywords: *ATP6V0A2* | cutis laxa | founder effect | haplotype analysis

ABSTRACT

ATP6V0A2-related cutis laxa is a rare autosomal recessive disorder characterized by connective tissue abnormalities, developmental delay, and neurological features. While multiple sequence variants have been reported, exon-level deletions are rarely documented, and their clinical significance remains largely unknown. This study aims to present the clinical and molecular characteristics of a novel frameshift variant and recurrent exon 16 deletions in the *ATP6V0A2* gene, to investigate a potential founder effect in southeastern Türkiye, and to contribute to the expanding genotype–phenotype correlation in *ATP6V0A2*-related cutis laxa. Ten cases from six unrelated families were evaluated. Exome sequencing, clinical exome sequencing, long-range polymerase chain reaction, gel electrophoresis, and haplotype analysis were performed. Variant interpretation followed ACMG and ClinGen guidelines. Clinical features were assessed through physical examination, developmental history, and neuroimaging. A novel homozygous frameshift variant (c.235del, p.Leu79Phefs*13) associated with severe neurological regression was identified in one case. Nine individuals carried a recurrent homozygous 380 bp deletion spanning exon 16 (c.1936-147_2055+113del). In our study, neurological regression—a feature rarely reported in the literature—was noted in two older patients. Haplotype analysis revealed shared homozygous regions in three cases, suggesting a founder effect. This cohort represents the largest reported series of *ATP6V0A2*-CL cases with exon 16 deletion to date. This study expands the genotypic and phenotypic spectrum of *ATP6V0A2*-CL and underscores the importance of copy number variation detection in next-generation sequencing-based diagnostics. The identification of a recurrent exon 16 deletion and shared haplotypes provides evidence for a founder effect in southeastern Türkiye and supports the implementation of population-specific screening for this variant.

1 | Introduction

Cutis laxa syndromes are rare genetic connective tissue disorders characterized by loose, excess skin and a prematurely aged appearance. Cutis laxa is also called elastolysis. Although cutis laxa syndromes have historically been grouped among segmental progeroid conditions due to their aged skin appearance, this classification does not imply generalized premature aging (Schnabel et al. 2021). According to data from the Rhône-Alpes EUROCAT registry, cutis laxa is an extremely rare disorder with an estimated prevalence of approximately 1 in 4 million (E. Robert, personal observation) (Van Maldergem et al. 1993).

ATP6V0A2-associated cutis laxa (*ATP6V0A2*-CL) is characterized by cutis laxa, findings associated with connective tissue disorders, developmental delay, and variable neurological findings. Among autosomal recessive subtypes, ATP6V0A2-related cutis laxa is considered one of the more frequently reported forms, despite its overall rarity. *ATP6V0A2*-CL has an autosomal recessive inheritance pattern. Clinically, *ATP6V0A2*-associated cutis laxa (*ATP6V0A2*-CL) presents with a multisystem phenotype involving dermatologic, neurologic, craniofacial, and systemic manifestations. Dermatologic findings include generalized or segmental cutis laxa with redundant, inelastic skin, delayed skin recoil, and prematurely aged facial appearance. Redundant skin folds, soft doughy texture, easy bruising, and Ehlers–Danlos-like atrophic scars are frequently reported. Skin laxity typically becomes less pronounced with age, consistent with previously described natural history patterns (Beyens et al. 2019). Neurologic features constitute a major disease component and may include global developmental delay, hypotonia, seizures, progressive neurological regression, and variable cognitive impairment. Brain MRI often demonstrates cortical and cerebellar malformations (e.g., pachygyria, cerebellar hypoplasia) and delayed myelination (Cohen et al. 2016; Azuri et al. 1999; Fischer et al. 2012). Craniofacial and dysmorphic features commonly include large or delayed-closing fontanelles, long philtrum, downslanting palpebral fissures, thick or coarse hair, frontal bossing, elongated facial shape, and characteristic periorbital skin redundancy. Additional findings may include strabismus, high myopia, corneal clouding, cataracts, and the distinctive ophthalmologic complication of Bruch's membrane rupture. Systemic findings reflect impaired connective tissue integrity and may include congenital hip dislocation, inguinal and umbilical hernias, joint laxity, and vascular abnormalities. Some individuals also present with skeletal anomalies or growth retardation (Van Maldergem et al. 1993). Individuals with *ATP6V0A2*-CL have a combined defect in *N*-glycosylation and *O*-glycosylation of serum proteins (Kornak et al. 2008). Serum sialotransferrin isoelectric focusing (IEF) and serum apolipoprotein C III IEF could demonstrate supportive laboratory findings (Van Maldergem et al. 1993). Cutis laxa, autosomal recessive, Type IIA and Wrinkly skin syndrome phenotypes were described in the *ATP6V0A2* gene (*OMIM** 611716).

The *ATP6V0A2* gene encodes the a2 subunit of the vacuolar H^+-ATPase (V-ATPase). V-ATPases are ATP-dependent proton pumps localized in cell and organelle membranes (Kornak et al. 2008; Nishi and Forgac 2002). V-ATPases are essential for acidification of diverse cellular components, including endosomes, lysosomes, clathrin-coated vesicles, secretory vesicles, secretion of tropoelastin, and regulation of protein transport and chromaffin granules (Smith et al. 2003; Guillard et al. 2009). Impaired secretion of certain brain or bone proteins with similar biochemical properties to tropoelastin has been suggested as a possible mechanism underlying the neural and skeletal defects in *ATP6V0A2*-CL (Hucthagowder et al. 2009).

The number of *ATP6V0A2*-CL-associated variants was reported as 59 in the Human Gene Mutation Database (HGMD): 20 missense/nonsense, 10 splicing, 18 small deletions, 7 small insertions, 3 gross deletions, and 1 gross insertion/duplication. Three gross deletions consist of 110 kb, 388 bp g.38642_39025 including exon 16, and exon 9 deletion (Hucthagowder et al. 2009; Stenson et al. 2020; Jones et al. 2013; Gardeitchik et al. 2014). To date, clinical information was described for six gross deletions in exon 16 (Fischer et al. 2012; Hucthagowder et al. 2009; Shishavan and Morovvati 2023).

In this study, we aimed to present the detailed clinical findings of a case with a novel frameshift variant associated with neurological decline, along with nine cases who have recurrent gross deletions in exon 16 of the *ATP6V0A2* gene. The study also aims to investigate a possible founder effect for the exon 16 deletion in cases with similar geographic backgrounds, southeastern Türkiye. To the best of our knowledge, we report the largest case series describing a gross deletion in the *ATP6V0A2* gene.

2 | Materials and Methods

2.1 | Clinical Evaluation

The cases were referred to Department of Medical Genetics for facial dysmorphism and developmental delay. The case files, findings, physical examination results, and family pedigrees were evaluated. The clinical evaluation of the case was conducted jointly by a clinical geneticist. Informed consent was obtained for the scientific use of the patients' data and photographs. Ethical approval for the study was obtained from the local ethics committee (decision number: 2024/111, date: **July 9, 2024).

2.2 | Exome Sequencing

Genomic DNA was isolated from peripheral blood samples using the QIAgen EZ1 instrument and the EZ1&2 DNA Blood 200 μL Kit. DNA concentration analysis was performed using Qubit (Thermo Fisher Scientific, USA). Exome sequencing (ES) was performed for Cases 1, 2, 3, 6, and 9, whereas Case 4 underwent clinical exome sequencing (CES). ES was conducted using the Roche KAPA HyperExome 96 rxn kit with MGI DNBSEQ-G400. Library preparation followed the manufacturer's protocol, including enzymatic fragmentation, end-repair/A-tailing, adaptor ligation, and target enrichment with KAPA HyperExome probes. Enriched libraries were amplified, quantified with Qubit, pooled equimolarly, and converted to single-stranded circular DNA for DNB preparation. Sequencing was carried out using paired-end 150 bp chemistry. FastQ files were analyzed using the Genomize SEQ platform, version 8.7.0. The CES study was performed with Illumina NextSeq 500/550 using the SOPHiA DDM Clinical Exome Solution v3 kit. Library preparation followed the manufacturer's protocol, including enzymatic fragmentation, end-repair/A-tailing, adapter ligation, and target enrichment by hybrid capture. Sequencing was conducted using paired-end chemistry (2 × 150 bp). CES data were analyzed with Sophia DDM V4. The reference of human genome was hg19/GRCh37.

2.3 | Variant Filtering and Interpretation

Variant prioritization was performed using a phenotype-driven approach. Given the strong clinical suspicion of cutis laxa,

Human Phenotype Ontology (HPO) terms related to cutis laxa (e.g., cutis laxa; HP:0000973) were used to define a virtual gene panel, and the analysis was directed toward genes known to be associated with cutis laxa and related connective tissue disorders, rather than an unrestricted genome-wide search (Gargano et al. 2024).

Pathogenic variant prioritization was performed by first excluding variants based on type, including synonymous, nonsense, missense, frameshift, splice site, indels, and in-frame changes. Subsequently, only rare variants with a minor allele frequency below 1% were retained, as determined by reference population databases such as 1000G (https://www.internationalgenome.org/), ExAC (https://exac.broadinstitute.org/), and gnomAD (https://gnomad.broadinstitute.org/) (Siva 2008; Lek et al. 2016; Chen et al. 2024). Sequencing data were visualized using the Integrative Genomics Viewer (IGV, https://software.broadinstitute.org/software/igv/) (Robinson et al. 2011). Variant pathogenicity classification was performed according to the American College of Medical Genetics and Genomics (ACMG) guidelines and ClinGen recommendations (Richards et al. 2015; Rehm et al. 2015).

2.4 | Long-Range Polymerase Chain Reaction and Gel Electrophoresis

Target regions were amplified using region-specific primers (forward: AGAAGGGGTGCTTGCCATA, reverse: GGCAACTTGTGACCATGGTT) via a long-range polymerase chain reaction (PCR) protocol. DNA fragmentation was carried out with the KAPA HyperPlus Kit (Roche, Basel, Switzerland). Adapter ligation was performed using the MGI Easy DNA Adapter-96 Plate Kit (MGI, Shenzhen, China), followed by a purification step with KAPA Hyper Pure Beads (Roche). The libraries were amplified using the MGI Primer Mix. Quantification of the libraries was performed using the Qubit 4 Fluorometer (Thermo Fisher Scientific), after which the samples were pooled. For single-stranded DNA (ssDNA) preparation, the MGIEasy Circularization Module (MGI) was used. Sequencing was carried out on the MGI DNBSEQ-G400 platform (MGI) using DNBSEQ-G400RS Sequencing Flow Cell and DNBSEQ-G400RS High-throughput Sequencing Kit (FCL PE150). For the deletion cases, variant confirmation and familial segregation analysis were performed using long-range PCR followed by gel electrophoresis. Long-range PCR data were analyzed with IGV. Gel electrophoresis was performed using the Cleaver Scientific nanoPAC-300P system.

2.5 | Sanger Sequencing

The frameshift variant identified in Case 1 was validated by Sanger sequencing. Genomic DNA was amplified using the following primers: Forward primer GCAGATCTCTCTAGGCAGCATT and reverse primer GACCCTGGGATGAGCTTTCT. Sequencing was performed using an ABI 3500XL Genetic Analyzer (Applied Biosystems, Foster City, CA, USA), and sequence traces were analyzed with CLC Genomics Workbench software.

2.6 | Haplotype Analysis

Haplotype analysis was performed for the cases carrying the homozygous deletion of exon 16 who underwent ES (Cases 2, 3, 6, and 9). The case analyzed by CES was not included in this analysis. Single-nucleotide polymorphisms (SNPs) were extracted from next-generation sequencing (NGS) data using VCF, BAM, and BAI files. SNPs were evaluated within a 19.8 Mb genomic interval (114,000,000–133,810,794), encompassing the *ATP6V0A2* gene. Shared haplotype data for the analyzed cases are presented in Tables S1 and S2.

3 | Results

The cohort comprised 10 individuals from six unrelated families. An equal sex distribution was observed, with five females and five males (50%, 5/10). Parental consanguinity was identified in all cases except one (Case 2), corresponding to a rate of 90% (9/10). Notably, six patients (60%, 6/10) were born preterm. Birth weight below −2 standard deviation scores (SDSs) for gestational age was recorded in four patients (40%, 4/10). Language developmental abnormalities were observed in six patients (60%, 6/10), and seven patients (70%, 7/10) were found to require special education support. Delayed acquisition of independent walking was reported in all cases (100%, 10/10). Physical examination revealed underweight in four patients (40%, 4/10), short stature in two (20%, 2/10), and microcephaly in nine (90%, 9/10). All patients (100%, 10/10) exhibited dysmorphic facial features (Figure 1). At initial evaluation, the diagnostic approach differed between Case 1 and the remaining patients. In Case 1, cutis laxa was not clinically apparent at presentation; therefore, genetic investigations were initiated primarily due to prominent facial dysmorphism and progressive neurological regression. In contrast, all other individuals were referred to medical genetics clinics because of facial dysmorphism and developmental delay, and the diagnosis of cutis laxa was subsequently established during the genetic evaluation based on characteristic skin findings. At the time of assessment, nine patients (excluding Case 1) exhibited clinically evident cutis laxa (Figure 1). In Case 1, retrospective review of infancy and childhood photographs revealed features consistent with cutis laxa, which had regressed over time. Two patients (20%, 2/10) had a history of seizures. While the seizures in Case 4 did not necessitate treatment, Case 9 was under antiepileptic medication. Developmental delay was present in all patients (100%, 10/10). Intellectual disability was observed in seven patients (70%, 7/10). Neurological decline was identified in two patients (20%, 2/10). Enlarged and delayed closure of fontanelles was observed in all patients (100%, 10/10). Detailed clinical features are summarized in Table 1. Detailed history and clinical findings of the patients are provided in the Supporting Information.

4 | Genetic Results

In Case 1, ES analysis revealed a homozygous c.235del p.(Leu79Phefs*13) variant in the *ATP6V0A2* gene. According to ACMG and ClinGen recommendations, the c.235del variant

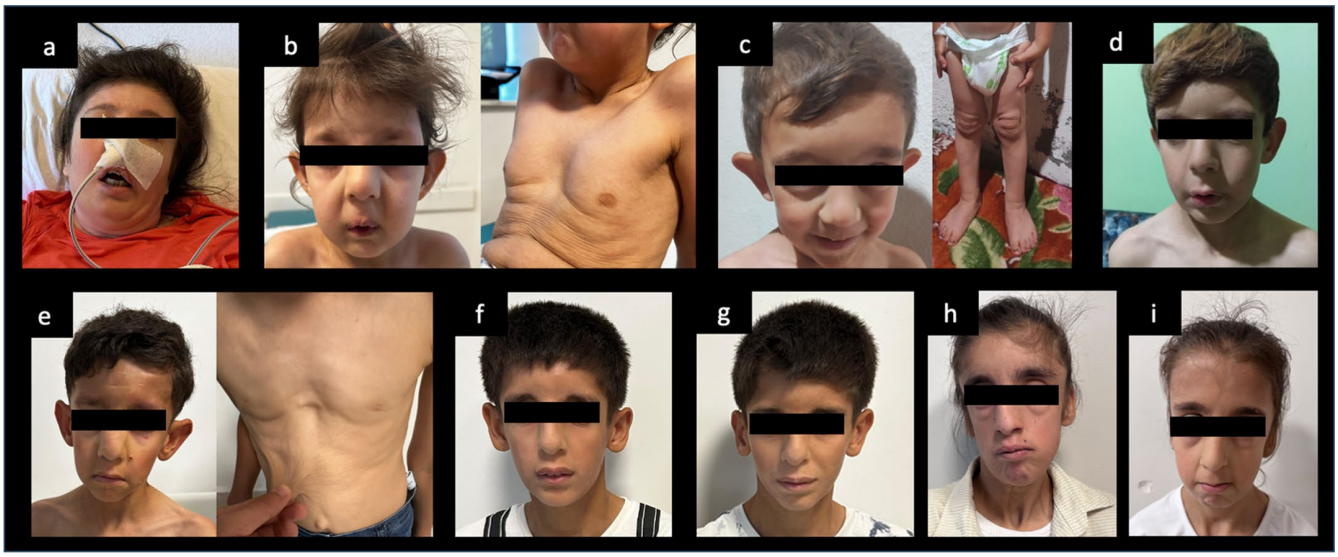

FIGURE 1 | Clinical photographs of individuals with *ATP6V0A2*-related cutis laxa demonstrate characteristic craniofacial and skin findings. Shared features across the cohort include periorbital skin laxity, downslanting palpebral fissures, midface hypoplasia, long philtrum, micrognathia, and low-set ears. (a) Case 1 shows brittle hair and strabismus. (b) Case 2 presents sparse brittle hair, excessive upper-eyelid folds, a tubular nose with anteverted nares, a whistling-like small mouth and loose skin. (c) Case 4 demonstrates gray sclerae, strabismus, a tubular nose, and loose skin. (d) Case 5 shows sparse brittle hair. (e) Case 6 exhibits coarse brittle hair, broad eyebrows, a broad nasal bridge, strabismus, large ears with simple helices, micrognathia, and loose skin. (f) Case 7 presents hypertelorism, gray sclerae, excessive upper-eyelid folds, a tubular nose, long smooth philtrum, and strabismus. (g) Case 8 shows hypertelorism, gray sclerae, excessive upper-eyelid folds, a tubular nose, and strabismus. (h) Case 9 demonstrates gray sclerae, a prominent nasal root, tubular nose with anteverted nares, midface hypoplasia, and loose redundant skin of the neck. (i) Case 10 shows hypertelorism, a prominent nasal root, tubular nose, and micrognathia.

was classified as pathogenic (PVS1, PM2, and PP4). Sanger sequencing was performed to confirm the variant and family segregations. Sanger sequencing confirmed the variant (Figure 2a). Sanger sequencing of the parents demonstrated a heterozygous c.235del variant in both.

In Cases 2, 3, 4, and 6, copy number variation analysis performed by ES and CES revealed a suspected homozygous deletion in exon 16 of the *ATP6V0A2* gene. To confirm the detected copy number losses, long-range PCR and gel electrophoresis were performed. A homozygous 380 bp deletion fully encompassing exon 16 of the *ATP6V0A2* gene was identified (c.1936-147_2055+113del, chr12: 124,235,510–124,235,889). In Cases 5, 7, 9, and 10, long-range PCR and gel electrophoresis were performed for diagnosis (Figure 2 and Supporting Information S2). For Case 9, post-diagnostic ES was performed to include the case in the haplotype analysis. Gross deletions in the *ATP6V0A2* gene are schematically illustrated in Figure 3. The clinical and molecular findings of exon 16 deletion cases in our cohort and those reported in the literature are summarized in Table 2.

5 | Haplotype Analysis Results

Pedigrees of all families are shown in Figure 4a, haplotype analysis could be performed only in cases with available ES data (Cases 2, 3, 6, and 9). Based on SNP analysis from the ES data, regions of homozygosity surrounding the *ATP6V0A2* gene were identified in Cases 2, 3, 6, and 9. The size of the homozygous region was determined to be 0.79 Mb (124,171,640–124,968,349) in Case 2, 42.2 Mb (82,751,167–124,979,833) in Case 3, 16.2 Mb (114,987,699–131,276,448) in Case 6, and 6.3 Mb (122,055,072–128,415,128) in Case 9. All four cases were found to share a common haplotype of 0.79 Mb spanning chr12: 124,171,640–124,968,349 (Figure 4). It was observed that Cases 3, 6, and 9 shared a common haplotype of 2.9 Mb (122,055,072–124,979,833). Cases 3 and 6 were found to share a larger shared haplotype of 9.9 Mb (114,987,699–124,979,833) (Figure 4b). The detailed haplotype analysis table is presented in Table S1.

6 | Discussion

ATP6V0A2-CL is an extremely rare syndrome, with fewer than 100 cases reported in the literature. In this study, we describe the largest reported cohort of individuals with *ATP6V0A2*-related cutis laxa carrying a novel homozygous exon 16 deletion, together with a novel frameshift variant associated with progressive neurological regression. Our findings expand the phenotypic and genotypic spectrum of *ATP6V0A2*-CL and provide evidence supporting a potential founder effect in southeastern Türkiye.

Morlino et al. reviewed *ATP6V0A2* cases published between 2005 and 2019, evaluating clinical data from 70 individuals across 65 families, and demonstrated marked heterogeneity in the age at diagnosis, which ranged from the neonatal period to 35 years of age (Morlino et al. 2021). Similarly, in our cohort, the age at diagnosis varied widely (3–26.5 years), underscoring the diagnostic heterogeneity of *ATP6V0A2*-related cutis laxa. This variability likely reflects differences in access to genetic testing and in clinical recognition of the phenotype, emphasizing the importance of increased awareness and timely referral for

TABLE 1 | Clinical and genetic findings of cases diagnosed with *ATP6V0A2* (NM_012463.4) related cutis laxa.

Family number	Family 1	Family 2	Family 3	Family 4	Family 4	Family 5	Family 5	Family 5	Family 6	Family 6
Case number	Case 1	Case 2	Case 3	Case 4	Case 5	Case 6	Case 7	Case 8	Case 9	Case 10
Gender	Female	Female	Female	Male	Male	Male	Male	Male	Female	Female
Age	26.5 years	3.5 years	16 years	5.5 years	3 years	5 years 11 months	11 years 9 months	11 years 9 months	14 years 5 months	9 years 3 months
Consanguinity	+	−	+	+	+	+	+	+	+	+
Variant type	Frameshift	Deletion	Deletion	Deletion	Deletion	Deletion	Deletion	Deletion	Deletion	Deletion
Exon	Exon 3	Exon 16	Exon 16	Exon 16	Exon 16	Exon 16	Exon 16	Exon 16	Exon 16	Exon 16
Zygosity	Homozygous	Homozygous	Homozygous	Homozygous	Homozygous	Homozygous	Homozygous	Homozygous	Homozygous	Homozygous
Nucleotide variation	c.235del	c.1936-147_2055+113del (exon 16 deletion)	c.1936-147_2055+113del (exon 16 deletion)	c.1936-147_2055+113del (exon 16 deletion)	c.1936-147_2055+113del (exon 16 deletion)	c.1936-147_2055+113del (exon 16 deletion)	c.1936-147_2055+113del (exon 16 deletion)	c.1936-147_2055+113del (exon 16 deletion)	c.1936-147_2055+113del (exon 16 deletion)	c.1936-147_2055+113del (exon 16 deletion)
Amino acid variation	p.L79Ffs*13	−	−	−	−	−	−	−	−	−
Clinvar accession number	SCV007127661	SCV007126672	SCV007126672	SCV007126672	SCV007126672	SCV007126672	SCV007126672	SCV007126672	SCV007126672	SCV007126672
Gestational week	30	40	40	40	32	40	32	32	28	36
Birth weight	1760 g (1.18 SD)	NA	2370 (−2.62 SD)	1700 g (−3.98 SD)	1500 g (−1.04 SD)	2750 g (−2.085 SD)	1620 g (−0.54 SD)	1700 g (−0.22 SD)	650 g (−2.68 SDS)	1900 g (−1.96 SDS)
Birth length	41 cm (0.72 SD)	NA	43 (−3.52 SD)	NA	NA	49 (−0.83 SD)	40 cm (−1.16 SD)	42 cm (−0.4 SD)	NA	NA
Birth occipito-facial circumference	NA	NA	30 (−3.63 SD)	NA	NA	NA	NA	NA	NA	NA
Start walking independently	30 months	24 months	16 months	30 months	36 months	21 months	24 months	24 months	36 months	30 months
Using first word	2 years	2 years	1 year	1 year	1 year	1.5 years	1 year	1 year	3 years	3 years
Language ability	Sentences including three–four words until the regression attacks	Sentences including two–three words	Normal	Sentences with two–three words	Sentences with two–three words	Normal	Normal	Normal	Articulation disorder	Articulation disorder
Psychiatric diagnosis	Bipolar disorder	−	−	Anxiety, fear of insects	Anxiety, fear of insects	−	−	−	−	−
Special education	+	+	+	Needs, but cannot reach	Needs, but cannot reach	−	−	−	+	+
Weight	71 kg (1.78 SDS)	13.9 kg (−0.68 SDS)	68.9 kg (1.83 SDS)	15 kg (−2.32 SDS)	12 kg (−1.98 SDS)	17.65 kg (−1.13 SDS)	31 kg (−1.6 SDS)	27 kg (−2.3 SDS)	33.65 kg (−3.83 SDS)	19.2 kg (−2.6 SDS)
Length	157 cm (−1.03 SDS)	95.6 cm (−0.85 SDS)	158.3 cm (−0.55 SDS)	105 cm (−2.06 SDS)	98 cm (−0.1 SDS)	117 cm (0.29 SDS)	150 cm (0.08 SDS)	145 cm (−0.62 SDS)	146 cm (−2.53 SDS)	126 cm (−1.31 SDS)

(Continues)

TABLE 1 | (Continued)

Occipito-facial circumference	50 cm (−4.91 SDS)	44.6 cm (−3.39 SDS)	49.3 cm (−4.62 SDS)	48 cm (−2.59 SDS)	48 cm (−1.53 SDS)	48.6 cm (−2.2 SDS)	49.2 cm (−3.65 SDS)	48.8 cm (−3.92 SDS)	50 cm (−4 SDS)	47.5 cm (−3.35 SDS)
Facial dysmorphism findings	Midface hypoplasia, long philtrum, hypertelorism, downslanting palpebral fissures, micrognathia, low-set ears, small mouth, high arched palate	Low anterior hairline, sparse eyebrows, hypertelorism, dowslanted palpebral fissures, gray scleras, excessive skin folds on upper palpebral fissures, prominent nasal root, tubular nose, anteverted nares, midface hypoplasia, long and smooth philtrum, downslanting palpebral fissures, micrognathia, small and whistling-like mouth, high arched palate, low-set and prominent ears, small ear lobules, hypoplastic antihelixes	Sparse and coarse hair pattern, sparse eyebrows, hypertelorism, dowslanted palpebral fissures, gray scleras, strabismus, prominent nasal root, tubular nose, anteverted nares, midface hypoplasia, downslanting palpebral fissures, small mouth, high arched palate, low-set ears	Broad eyebrows, downslating palpebral fissures, tubular nose, long philtrum, low set and large ears, micrognathia, small mouth, high arched palate	Broad eyebrows, downslating palpebral fissures, strabismus, long philtrum, low set and large ears, micrognathia, small mouth, high arched palate	Broad eyebrows, downslating palpebral fissures, broad nasal bridge, long philtrum, large ears and simple folded helices, micrognathia, high arched palate	Broad eyebrows, downslating palpebral fissures, broad nasal bridge, long philtrum, low set ears, large ears and simple folded helices, micrognathia, small mouth, high arched palate	Broad eyebrows, downslating palpebral fissures, broad nasal bridge, long philtrum, low set ears, large ears and simple folded helices, micrognathia, small mouth, high arched palate	Hypertelorism, dowslanted palpebral fissures, gray scleras, excessive skin folds on upper palpebral fissures, prominent nasal root, tubular nose, anteverted nares, midface hypoplasia, long and smooth philtrum, micrognathia, small and whistling-like mouth, high arched palate, low-set ears	Hypertelorism, dowslanted palpebral fissures, gray scleras, excessive skin folds on upper palpebral fissures, prominent nasal root, tubular nose, anteverted nares, midface hypoplasia, long and smooth philtrum, micrognathia, small and whistling-like mouth, high arched palate, low-set ears
Skin	Cutis laxa, loose redundant skin and excessive skin folds in infant and childhood period, loose redundant skin, multiple nevus on back	Cutis laxa, loose and redundant skin, excessive skin folds	Lipodystrophy, cutis laxa, loose and redundant skin	Cutis laxa, loose and redundant skin	Cutis laxa, loose and redundant skin	Lipodystrophy, cutis laxa, loose and redundant skin	Lipodystrophy, cutis laxa, loose and redundant skin	Lipodystrophy, cutis laxa, loose and redundant skin	Cutis laxa, loose and redundant skin	Cutis laxa, loose and redundant skin
Nails	Normal	Normal	Brittle, slow growth	Normal	Normal	Normal	Normal	Normal	Normal	Normal
Hair	Brittle hair, poor hair growth	Sparse, brittle hair	Coarse hair, brittle hair	Sparse, brittle hair	Sparse, brittle hair	Coarse and brittle hair	Coarse and brittle hair	Coarse and brittle hair	Coarse hair, brittle hair	Coarse hair, brittle hair

(Continues)

TABLE 1 | (Continued)

Teeth	Orthodontic treatment due to malocclusion	Dental caries	Dental caries	Dental caries	Dental caries	Dental caries	Dental caries	Dental caries	Dental caries	Dental caries
Neurological signs	Bedridden, muscle weakness, bilateral positive Babinski sign, inability to speak, 2/3 positive deep tendon reflexes	Learning disabilities	Gait disturbance, frequent falls, learning disabilities	–	–	Gait disturbance, frequent falls	Wide-based gait	Wide-based gait	–	Gait disturbance, frequent falls
Seizure	–	–	–	Seizures for three times, no treatment needed	–	–	–	–	+	–
Ataxia	+	–	+	–	–	–	–	–	–	–
EEG	Normal	NA	Normal	NA	NA	Normal	Normal	Normal	+ (increased fast background activity)	Normal
Brain MRI findings	Cerebellar atrophy, in SWI examination, signal less areas secondary to the accumulation of paramagnetic material were noted in the bilateral putamen, globus pallidus, substantia nigra, and nucleus ruber, wide lateral ventricles, third ventricle and hemispheric cortical sulci	Normal	Signal residual foci in the subcortical white matter showing diffusion restriction in the right parietotemporal lobe, asymmetric dilatation in the temporal horn of the right lateral ventricle, atrophy and increased signal in the hippocampus, cortical dysplasia in the right frontal region	NA	NA	Mega cisterna magna	Normal	Normal	Dilatation of fourth ventricle	NA
Eye anomalies	Strabismus, myopia	Normal	Myopia (8/8), keratoconus, strabismus	–	Strabismus	Strabismus, myopia, astigmatism, entropion	Strabismus, entropion, myopia	Strabismus, entropion, myopia	Entropion	Entropion
Hypotonia	+	+	+	+	+	+	+	+	+	+
Developmental delay/ intellectual disability	+/+	+/+	+/+	+/+	+/+	+/–	+/–	+/–	+/+	+/+

(Continues)

TABLE 1 | (Continued)

Neurological decline	+	−	+	−	−	−	−	−	−	−
Hypermobile joints	+	+	+	+	+	+	+	+	+	+
Enlarged fontanels/ delayed closure	+/+	+/+	+/+	+/+	+/+	+/+	+/+	+/+	+/+	+/+
Congenital dislocation of hips	+	+	+	−	−	−	−	+	−	−
Inguinal hernia	−	+	+	−	−	+	−	+	−	−
Cardiovascular system		Normal	Mild left ventricular hypertrophy, ascending aorta diameter was 21 cm	Congenital heart defect, unknown type	Congenital heart defect, unknown type	NA	Normal	Normal	Normal	Normal
Gastrointestinal system	Choledocholithiasis	Normal	Hepatosteatosis	Constipation	Constipation	−	−	−	Normal	Normal
Genitourinary system		Mild left pelviectasis	Kidney failure	Undescended testes	Undescended testes	Undescended testes and inguinal hernia	Hypospadias	Cryptorchidism	Normal	Normal
Maternal age at birth	25 years	32	Normal	21	23	33	29	29	20	25
Paternal age at birth	23 years	35	19	25	27	35	29	29	22	27
Other clinical findings	Echolalia, hyperacusis	−	−	Frequent epistaxis	−	Hyperacusis	−	−	Flexion contractures of the distal interphalangeal joints of the fingers, pectus carinatum	Flexion contractures of the distal interphalangeal joints of the fingers

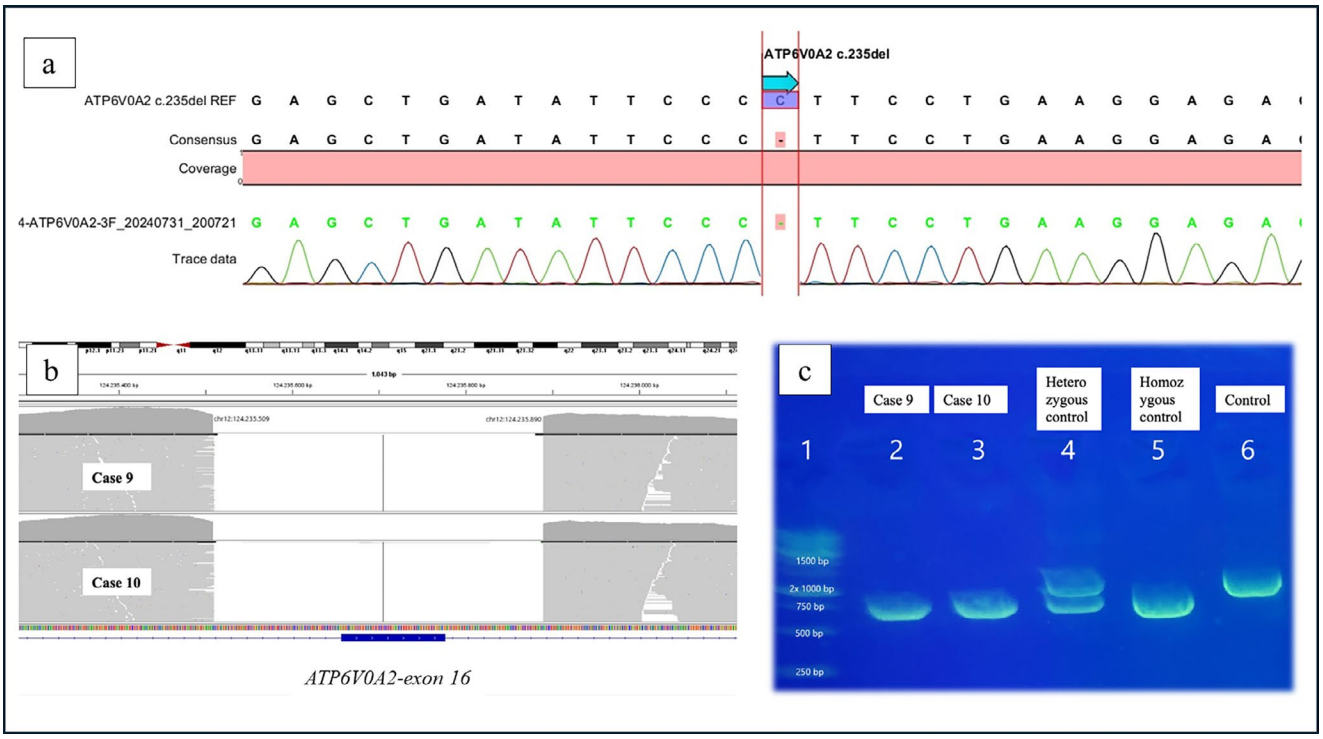

FIGURE 2 | Integrated molecular characterization of *ATP6V0A2* variants. (a) Sanger chromatogram from Case 1 confirming the frameshift variant c.235del (p.Leu79Phefs*13). (b) Long-range PCR-based sequencing view on IGV from Case 9 and Case 10 demonstrates loss of aligned reads and a defined breakpoint interval consistent with an exon 16 deletion. (c) Agarose gel electrophoresis of Cases 9 and 10 shows the expected deletion band alongside heterozygous, homozygous, and negative controls.

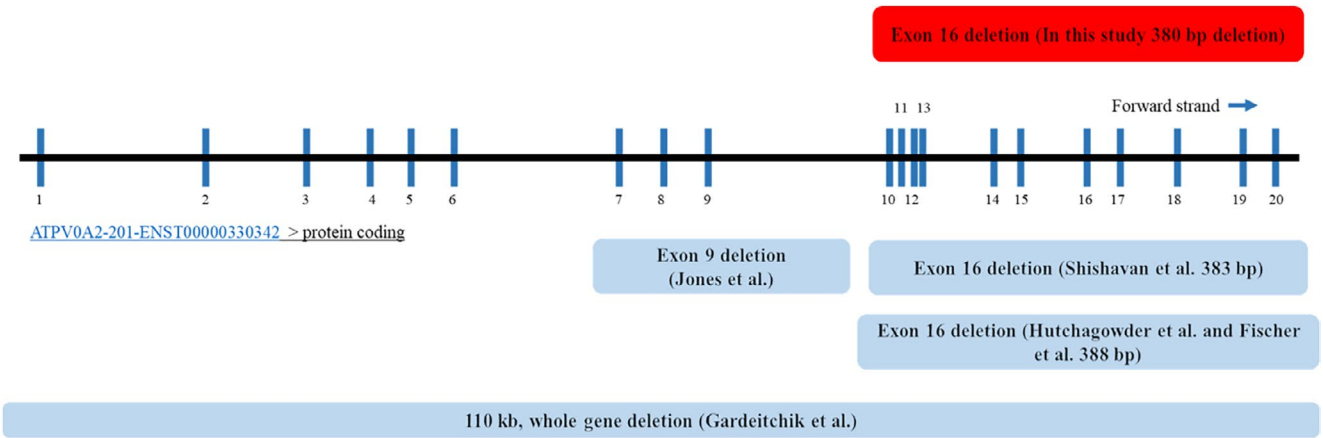

FIGURE 3 | Gross deletions in the *ATP6V0A2* gene reported in the literature and identified in the present study. Previously reported deletions included exon 9 deletion (Jones et al.), exon 16 deletions of different sizes (Hutchagowder et al., Fischer et al., and Shishavan et al.), and a 110 kb whole-gene deletion (Gardeitchik et al.). The exon 16 deletion identified in the present study (380 bp) is highlighted in red.

molecular diagnosis. While the review reported a slight male predominance (female; 41%, male; 59%), our cohort showed an equal sex distribution.

All our cases with the *ATP6V0A2* gene variant had hypotonia and delayed walking. All cases acquired walking ability between 16 and 36 months. Although walking ability was acquired, most of them continued to have gait abnormalities and frequent falls. All of these cases had distinct cutis laxa symptoms starting in infancy. Early cutis laxa and hypotonia in these cases may be supportive findings for the early diagnosis.

van Maldergem et al. described cognitive decline following seizures in many cases, and one case developed neurological regression that led to bedriddenness without seizures. In this case a bedridden state occurred after 16 years in their patient (Van Maldergem et al. 2008). In our study, neurological regression was detected in Cases 1 and 3. ES was performed in both cases, and no second variant was identified that could explain the neurological regression. In Case 1, significant life-limiting neurological and psychiatric findings emerged, and neurological regression occurred. She presented bipolar disorder at the age of 18, loss of balance started at the age of 20, and attacks of unilateral weakness

TABLE 2 | Phenotypic spectrum of biallelic *ATP6V0A2* exon 16 deletions: Published cases and the current cohort.

Case number	Case 2	Case 3	Case 4	Case 5	Case 6	Case 7	Case 8	Case 9	Case 10
Zygosity	Homozygous	Homozygous	Homozygous	Homozygous	Homozygous	Homozygous	Homozygous	Homozygous	Homozygous
Nucleotide variation	c.1936-147_2055+113del	c.1936-147_2055+113del	c.1936-147_2055+113del	c.1936-147_2055+113del	c.1936-147_2055+113del	c.1936-147_2055+113del	c.1936-147_2055+113del	c.1936-147_2055+113del	c.1936-147_2055+113del
Microcephaly	+	+	+	−	+	+	+	+	+
Cutis laxa or wrinkled skin	+	+	+	+	+	+	+	+	+
Seizure	−	−	+	−	−	−	−	+	−
Positive brain MRI findings	−	+	NA	NA	+	−	−	+	NA
Eye anomalies	−	+	−	+	+	+	+	+	+
Developmental delay/intellectual disability	+/+	+/+	+/+	+/+	+/−	+/−	+/−	+/+	+/+
Hypermobile joints	+	+	+	+	+	+	+	+	+
Enlarged fontanels or delayed closure	+	+	+	+	+	+	+	+	+

Case number	Hucthagowder et al. (2009) P2, Iran	Hucthagowder et al. (2009) P4, Türkiye	Hucthagowder et al. (2009) P9, Türkiye	Hucthagowder et al. (2009) P10, Türkiye	Fischer et al. (2012) P12, Türkiye	Shishavan and Morovvati (2023) Iran
Zygosity	Homozygous	Homozygous	Homozygous	Homozygous	Homozygous	Homozygous
Nucleotide variation	c.1936_2055del	c.1936_2055del	c.1936_2055del	c.1936_2055del	c.1936_2055del	c.1936-147_2055+116del
Microcephaly	+	+	+	−	NA	NA
Cutis laxa or wrinkled skin	+	+	+	+	+	+
Seizure	−	−	−	−	NA	NA
Positive brain MRI findings	NA	NA	+	+	NA	NA
Eye anomalies	+	+	+	+	NA	+
Developmental delay/intellectual disability	+/+	−/−	+/+	+/+	NA/+ (very mild)	−/+
Hypermobile joints	+	+	+	+	+	+
Enlarged fontanels or delayed closure	+	+	+	+	+	NA

Abbreviations: "+" indicates that the feature was reported; "−" indicates not reported; NA, not available/not assessed in the original publication or not documented in the medical record.

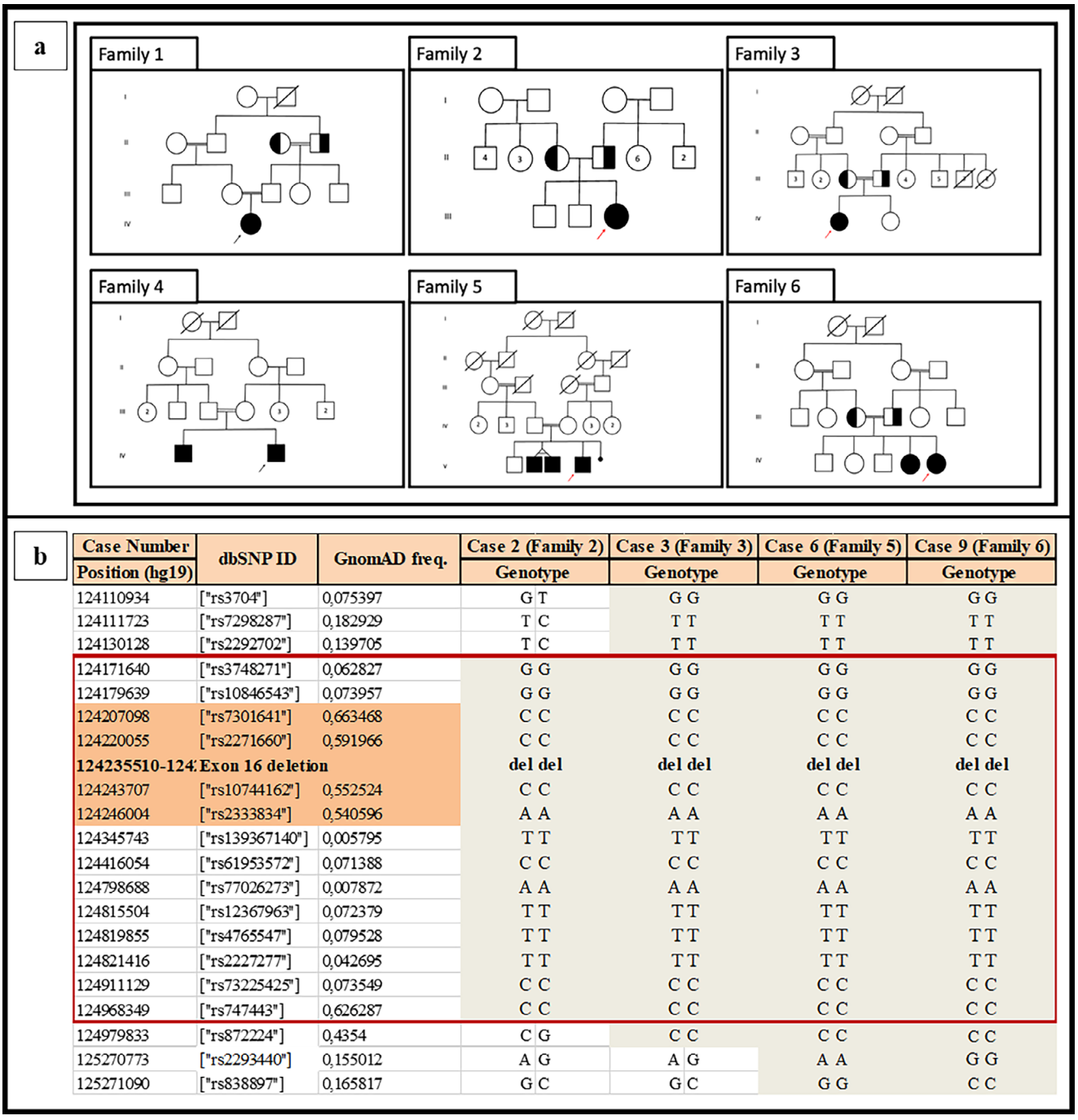

b

Case Number	dbSNP ID	GnomAD freq.	Case 2 (Family 2)	Case 3 (Family 3)	Case 6 (Family 5)	Case 9 (Family 6)
Position (hg19)			Genotype	Genotype	Genotype	Genotype
124110934	["rs3704"]	0,075397	G T	G G	G G	G G
124111723	["rs7298287"]	0,182929	T C	T T	T T	T T
124130128	["rs2292702"]	0,139705	T C	T T	T T	T T
124171640	["rs3748271"]	0,062827	G G	G G	G G	G G
124179639	["rs10846543"]	0,073957	G G	G G	G G	G G
124207098	["rs7301641"]	0,663468	C C	C C	C C	C C
124220055	["rs2271660"]	0,591966	C C	C C	C C	C C
124235510-124	**Exon 16 deletion**		**del del**	**del del**	**del del**	**del del**
124243707	["rs10744162"]	0,552524	C C	C C	C C	C C
124246004	["rs2333834"]	0,540596	A A	A A	A A	A A
124345743	["rs139367140"]	0,005795	T T	T T	T T	T T
124416054	["rs61953572"]	0,071388	C C	C C	C C	C C
124798688	["rs77026273"]	0,007872	A A	A A	A A	A A
124815504	["rs12367963"]	0,072379	T T	T T	T T	T T
124819855	["rs4765547"]	0,079528	T T	T T	T T	T T
124821416	["rs2227277"]	0,042695	T T	T T	T T	T T
124911129	["rs73225425"]	0,073549	C C	C C	C C	C C
124968349	["rs747443"]	0,626287	C C	C C	C C	C C
124979833	["rs872224"]	0,4354	C G	C C	C C	C C
125270773	["rs2293440"]	0,155012	A G	A G	A A	G G
125271090	["rs838897"]	0,165817	G C	G C	G G	C C

FIGURE 4 | (a) Pedigrees of families with *ATP6V0A2* variants. Pedigrees of all families are shown. The probands marked with the red arrow indicate the cases included in the haplotype analysis. Filled symbols indicate affected individuals and half-filled symbols indicate heterozygous carriers. (b) The figure shows the SNPs used in homozygosity and haplotype analyses performed on the cases. The areas highlighted with a cream background indicate the SNPs found to be homozygous. The region marked with a red frame represents the shared SNPs around the *ATP6V0A2* gene observed in all four cases. The region highlighted in orange indicates the SNPs located within the *ATP6V0A2* gene.

and inability to speak started at the age of 24, lasting 20–30 min; by the age of 26, she had progressed to a bedridden state. In Case 3, neurological regression started at the age of 14 with ataxic gait and gait deterioration and has been continuing for the last 2 years. In addition, brain MRI findings were present in Cases 1 and 3. No brain MRI findings were detected in the other cases where brain MRI findings were available. Consistent with this finding, van Maldergem et al. associated this regression with brain imaging findings, including cerebral atrophy (Van Maldergem et al. 1993).

According to HGMD and GeneReviews, copy number variants involving *ATP6V0A2* are rare, with more than 95% of reported pathogenic variants being sequence-level changes and fewer than 5% detected by deletion/duplication analyses. Consequently, clinical data on individuals carrying *ATP6V0A2* deletions remain limited (Van Maldergem et al. 1993; Stenson et al. 2020). To the best of our knowledge, there are six cases with homozygous gross deletion of the *ATP6V0A2* gene whose clinical information is currently available. Four of these cases are from Türkiye and two are from

Iran (Fischer et al. 2012; Hucthagowder et al. 2009; Shishavan and Morovvati 2023). We therefore provide a targeted comparison of published exon 16 deletion cases with our cohort in Table 2. Although the reported deletions also encompassed exon 16, the breakpoints differed from those identified in our study. Given the geographic proximity of Türkiye and Iran, the recurrence of exon 16 deletions in both countries is compatible with the possibility of shared ancestral alleles and a common regional haplotype.

Overall, the clinical phenotype observed in our cohort of individuals with homozygous exon 16 deletions of *ATP6V0A2* was largely consistent with previously reported cases carrying similar gross deletions. Notably, seizure frequency appeared to be low in both our cohort and previously published exon 16 deletion cases. In the review published by Morlino et al., seizures were reported in 21 out of 71 cases (Morlino et al. 2021). In GeneReviews, seizure frequency was reported as 100%. The seizure frequency in our cases with exon 16 deletion and in previously reported cases was much lower than in cases carrying other variants of the *ATP6V0A2* gene (Van Maldergem et al. 1993). However, given the limited number of reported cases, this observation should be interpreted cautiously and warrants confirmation in larger cohorts.

The identification of extended regions of homozygosity encompassing the *ATP6V0A2* gene in Cases 2, 3, and 6 suggests the possibility of parental consanguinity and/or a shared ancestral haplotype. Notably, the presence of such a region in Case 2, despite the absence of reported parental consanguinity, further supports a potential founder effect given the family's origin from southeastern Türkiye. The greater extent of the shared haplotype observed in Cases 3 and 6 indicates a more recent common ancestry. Despite the lack of haplotype data from previously reported cases in Türkiye and Iran, future haplotype analyses may reveal a shared common ancestral variant, which would provide stronger evidence for a founder effect in this population. These findings, particularly the recurrent identification of deletions involving exon 16 in apparently unrelated individuals from the same geographic region, support the possibility of a founder effect. In rare autosomal recessive disorders, especially when structural variants are suspected but not initially detected by standard variant calling pipelines, ES-based identification of homozygous regions can serve as a valuable diagnostic clue. The large-shared haplotype observed in our cohort further reinforces the likelihood of a common ancestral origin.

In our cohort, the preliminary diagnosis was established through ES-based CNV analysis in all cases except for Cases 9 and 10. These diagnoses were further validated by PCR and gel electrophoresis. This underscores the critical role of CNV detection in NGS-based diagnostic workflows for *ATP6V0A2*-CL. For Cases 9 and 10, long-range PCR and gel electrophoresis were employed as the primary diagnostic tools due to their origin from a geographic region where previously diagnosed cases had been identified, thereby eliminating the need for NGS-based approaches. While microarray and multiplex ligation-dependent probe amplification (MLPA) are well-established techniques for identifying copy number alterations, we highlight the diagnostic utility and cost-effectiveness of PCR assays using primers specifically designed for individuals from the suspected founder effect region. This approach may be particularly advantageous in resource-limited settings or in populations with known recurrent deletions.

7 | Limitations and Future Directions

Our most important limitation was the lack of follow-up data because some of our cases were young. Due to the unavailability of ES data for Family 4, this family could not be included in the homozygosity mapping and haplotype analyses. Future investigations should aim to define the clinical implications of the founder effect more comprehensively and strengthen genotype–phenotype correlations to support therapeutic development.

8 | Conclusion

In the following studies, limited information was provided on both cognitive decline that develops after seizures and neurological regression that begins with a nonseizure attack that leads to bedridden patients. More studies and follow-ups are needed on which *ATP6V0A2* gene variants show neurological decline and by which mechanism. We suggest that age may influence these findings. Our cases were diagnosed through ES-based CNV analysis, highlighting the necessity of incorporating CNV detection into routine NGS diagnostics. This is particularly crucial for *ATP6V0A2*-related cutis laxa, where structural variants such as exon-level deletions may be under-recognized if CNV analysis is not performed. In addition, we emphasize the diagnostic utility and cost-effectiveness of long-range PCR and gel electrophoresis using region-specific primers, particularly in populations residing in areas with suspected founder effects. The potential identification of a shared ancestral haplotype among cases from Türkiye and Iran would provide compelling evidence for a founder effect, highlighting the importance of haplotype analysis in elucidating the genetic basis of recurrent deletions in consanguineous and geographically clustered populations.

Author Contributions

Z.E. performed and interpreted the genetic tests, clinical examinations, wrote the manuscript, and collected data. M.Ö., E.H., H.B., E.B., and A.T.-Ü. performed and interpreted the genetic tests and clinical examinations. Z.E. and A.S. make haplotype analysis. G.Ü.-B. wrote the manuscript and psychiatric evaluations. F.E. provided support for neurological examinations.

Acknowledgments

The authors thank the patients and families for their participation in this study. We also extend our gratitude to the Clinical Genetics Clinics and their teams who contributed to patient referral and data sharing. Their valuable collaboration made this study possible.

Conflicts of Interest

The authors declare no conflicts of interest.

Data Availability Statement

The data that support the findings of this study are available on request from the corresponding author. The data are not publicly available due to privacy or ethical restrictions.

References

Azuri, J., A. Mizrachi, S. Weintraub, and T. Lerman-Sagie. 1999. "Neurological Involvement in a Child With the Wrinkly Skin Syndrome." *American Journal of Medical Genetics* 82, no. 1: 31–33.

Beyens, A., E. Moreno-Artero, C. Bodemer, et al. 2019. "ATP6V0A2-Related Cutis Laxa in 10 Novel Patients: Focus on Clinical Variability and Expansion of the Phenotype." *Experimental Dermatology* 28, no. 10: 1142–1145.

Chen, S., L. C. Francioli, J. K. Goodrich, et al. 2024. "A Genomic Mutational Constraint Map Using Variation in 76,156 Human Genomes." *Nature* 625, no. 7993: 92–100.

Cohen, R., A. Halevy, S. Aharoni, et al. 2016. "Polymicrogyria and Myoclonic Epilepsy in Autosomal Recessive Cutis Laxa Type 2A." *Neurogenetics* 17, no. 4: 251–257.

Fischer, B., A. Dimopoulou, J. Egerer, et al. 2012. "Further Characterization of *ATP6V0A2*-Related Autosomal Recessive Cutis Laxa." *Human Genetics* 131, no. 11: 1761–1773.

Gardeitchik, T., M. Mohamed, B. Fischer, et al. 2014. "Clinical and Biochemical Features Guiding the Diagnostics in Neurometabolic Cutis Laxa." *European Journal of Human Genetics* 22, no. 7: 888–895.

Gargano, M. A., N. Matentzoglu, B. Coleman, et al. 2024. "The Human Phenotype Ontology in 2024: Phenotypes Around the World." *Nucleic Acids Research* 52, no. D1: D1333–D1346.

Guillard, M., A. Dimopoulou, B. Fischer, et al. 2009. "Vacuolar H+-ATPase Meets Glycosylation in Patients With Cutis Laxa." *Biochimica et Biophysica Acta, Molecular Basis of Disease* 1792, no. 9: 903–914.

Hucthagowder, V., E. Morava, U. Kornak, et al. 2009. "Loss-of-Function Mutations in *ATP6V0A2* Impair Vesicular Trafficking, Tropoelastin Secretion and Cell Survival." *Human Molecular Genetics* 18, no. 12: 2149–2165.

Jones, M. A., D. Rhodenizer, C. da Silva, et al. 2013. "Molecular Diagnostic Testing for Congenital Disorders of Glycosylation (CDG): Detection Rate for Single Gene Testing and Next Generation Sequencing Panel Testing." *Molecular Genetics and Metabolism* 110, no. 1–2: 78–85.

Kornak, U., E. Reynders, A. Dimopoulou, et al. 2008. "Impaired Glycosylation and Cutis Laxa Caused by Mutations in the Vesicular H^+-ATPase Subunit ATP6V0A2." *Nature Genetics* 40, no. 1: 32–34.

Lek, M., K. J. Karczewski, E. V. Minikel, et al. 2016. "Analysis of Protein-Coding Genetic Variation in 60,706 Humans." *Nature* 536, no. 7616: 285–291.

Morlino, S., G. Nardella, S. Castellana, et al. 2021. "Review of Clinical and Molecular Variability in Autosomal Recessive Cutis Laxa 2A." *American Journal of Medical Genetics Part A* 185, no. 3: 955–965.

Nishi, T., and M. Forgac. 2002. "The Vacuolar (H^+)-ATPases–Nature's Most Versatile Proton Pumps." *Nature Reviews Molecular Cell Biology* 3, no. 2: 94–103.

Rehm, H. L., J. S. Berg, L. D. Brooks, et al. 2015. "ClinGen—The Clinical Genome Resource." *New England Journal of Medicine* 372, no. 23: 2235–2242.

Richards, S., N. Aziz, S. Bale, et al. 2015. "Standards and Guidelines for the Interpretation of Sequence Variants: A Joint Consensus Recommendation of the American College of Medical Genetics and Genomics and the Association for Molecular Pathology." *Genetics in Medicine* 17, no. 5: 405–424.

Robinson, J. T., H. Thorvaldsdottir, W. Winckler, et al. 2011. "Integrative Genomics Viewer." *Nature Biotechnology* 29, no. 1: 24–26.

Schnabel, F., U. Kornak, and B. Wollnik. 2021. "Premature Aging Disorders: A Clinical and Genetic Compendium." *Clinical Genetics* 99, no. 1: 3–28.

Shishavan, N. S., and S. Morovvati. 2023. "A Novel Deletion Mutation in the ATP6V0A2 Gene in an Iranian Patient Affected by Autosomal Recessive Cutis Laxa." *Irish Journal of Medical Science* 192, no. 5: 2279–2282.

Siva, N. 2008. "1000 Genomes Project." *Nature Biotechnology* 26, no. 3: 256.

Smith, A. N., R. C. Lovering, M. Futai, J. Takeda, D. Brown, and F. E. Karet. 2003. "Revised Nomenclature for Mammalian Vacuolar-Type H^+-ATPase Subunit Genes." *Molecular Cell* 12, no. 4: 801–803.

Stenson, P. D., M. Mort, E. V. Ball, et al. 2020. "The Human Gene Mutation Database (HGMD®): Optimizing Its Use in a Clinical Diagnostic or Research Setting." *Human Genetics* 139, no. 10: 1197–1207.

Van Maldergem, L., W. Dobyns, and U. Kornak. 1993. "ATP6V0A2-Related Cutis Laxa." In *GeneReviews®*, edited by M. P. Adam, S. Bick, G. M. Mirzaa, R. A. Pagon, S. E. Wallace, and A. Amemiya. University of Washington.

Van Maldergem, L., M. Yuksel-Apak, H. Kayserili, et al. 2008. "Cobblestone-Like Brain Dysgenesis and Altered Glycosylation in Congenital Cutis Laxa, Debre Type." *Neurology* 71, no. 20: 1602–1608.

Supporting Information

Additional supporting information can be found online in the Supporting Information section. **Data S1:** ajmga70102-sup-0001-Supinfo.docx. **Data S2:** ajmga70102-sup-0002-Figures.docx. **Data S3:** ajmga70102-sup-0003-Tables.docx.